N-d scattering above the deuteron breakup threshold

A. Kievsky,[1] M. Viviani,[1] and S. Rosati[1,2]
[1]*Istituto Nazionale di Fisica Nucleare, Piazza Torricelli 2, 56100 Pisa, Italy*
[2]*Dipartimento di Fisica, Universita' di Pisa, Piazza Torricelli 2, 56100 Pisa, Italy*
(Received 28 May 1997)

The complex Kohn variational principle and the (correlated) hyperspherical harmonics technique are applied to study *N-d* scattering above the deuteron breakup threshold. The configuration with three outgoing nucleons is explicitly taken into account by solving a set of differential equations with outgoing boundary conditions. A convenient procedure is used to obtain the correct boundary conditions at values of the hyperradius of ≈ 100 fm. The inclusion of the Coulomb potential is straightforward and does not give additional difficulties. Numerical results have been obtained for a simple *s*-wave central potential. They are in nice agreement with the benchmarks produced by different groups using the Faddeev technique. Comparisons are also done with experimental elastic *N-d* cross section at several energies. [S0556-2813(97)00812-1]

PACS number(s): 25.10.+s, 03.65.Nk, 13.75.Cs, 25.55.Ci

One of the main objectives in nuclear physics is knowledge of the nuclear interaction. In practice, the two-nucleon scattering data are used to determine the on-shell nucleon-nucleon (NN) interaction. The off-shell properties of nuclear potentials and many-body force contributions must be tested in systems with $A>2$. As a consequence, much work has to be devoted to the understanding of the three-nucleon bound and scattering states. The Faddeev theory has been extensively applied to this problem and, in particular, to the study of the *n-d* scattering under and above the deuteron breakup threshold. The corresponding Faddeev equations in momentum space were originally solved by Kloet and Tjon [1] for a central *s*-wave potential. At present, different numerical techniques are available to solve the Faddeev equations in configuration and momentum space. In Refs. [2,3] benchmark calculations for *n-d* scattering were given as reference for new techniques. Realistic potentials have been used to calculate the *n-d* scattering cross section at different energies [4]. For the *p-d* channel many accurate experimental data are available, but the Faddeev approach to this process becomes difficult due to the Coulomb repulsion [5–7]. Such a difficulty is not present in the variational technique developed in Ref. [8] for the *N-d* scattering below the deuteron breakup threshold. The extension of this above the deuteron breakup threshold is the object of the present paper. In particular, the asymptotic conditions to describe three outgoing nucleons in the *n-n-p* and *p-p-n* states are explicitly taken into account.

In the following the important aspects of the approach are briefly outlined and various results obtained for a simple *s*-wave central potential are reported. More details on the adopted procedures and results for realistic potentials will be presented in a forthcoming paper [9].

Following Ref. [8], the wave function of the system is written as a sum of two terms:

$$\Psi = \Psi_C + \Psi_A . \tag{1}$$

The Ψ_A term is a solution of the Schrödinger equation in the asymptotic region where the incident nucleon and the deuteron are well apart. The Ψ_C term must guarantee an accurate description of the system when the three nucleons are close to each other; moreover, for large interparticle separations it has to describe the breakup configurations. Ψ_C is written as a sum of channel contributions, labeled by the angular-spin-isospin quantum number. The associated two-dimensional spatial amplitudes are expanded in terms of the pair correlated hyperspherical harmonic (PHH) basis [10].

The wave function corresponding to an asymptotic state ${}^{(2S+1)}L_J$ has the form

$$\Psi_{LSJ} = \sum_{i=1,3} \left[\Psi_C(\mathbf{x}_i,\mathbf{y}_i) + \Omega^{\rm in}_{LSJ}(\mathbf{x}_i,\mathbf{y}_i) - \sum_{L'S'} {}^J\mathcal{S}^{SS'}_{LL'} \Omega^{\rm out}_{L'S'J}(\mathbf{x}_i,\mathbf{y}_i) \right], \tag{2}$$

where the summation is extended over the three different choices of the Jacobi coordinates $(\mathbf{x},\mathbf{y})$. L is the relative angular momentum between the incident nucleon and the deuteron, S is the spin obtained by coupling the spin $j=1$ of the deuteron with spin 1/2 of the third nucleon, and J is the total angular momentum of the system. ${}^J\mathcal{S}^{SS'}_{LL'}$ are the collision-matrix ($\mathcal{S}$-matrix) elements describing the $2\rightarrow 2$ elastic scattering. The function Ω^{λ}_{LSJ} is the ingoing ($\lambda \equiv$ in) or the outgoing ($\lambda \equiv$ out) solution of the two-body *N-d* Schrödinger equation in the asymptotic region. These solutions contain suitable regularizing factors at small distances. The explicit form of Ψ_C is

$$\Psi_C(\mathbf{x}_i,\mathbf{y}_i) = \sum_\alpha \phi_\alpha(x_i,y_i)\mathcal{Y}_\alpha(jk,i), \tag{3}$$

$$\mathcal{Y}_\alpha(jk,i) = \{[Y_{\ell_\alpha}(\hat{x}_i)Y_{L_\alpha}(\hat{y}_i)]_{\Lambda_\alpha}[s^{jk}_\alpha s^i_\alpha]_{S_\alpha}\}_{JJ_z}[t^{jk}_\alpha t^i_\alpha]_{TT_z}, \tag{4}$$

 © 1997 The American Physical Society

$$\phi_\alpha(x_i,y_i)=\rho^{\ell_\alpha+L_\alpha}f_\alpha(x_i)\left[\sum_k u_k^\alpha(\rho)^{(2)}P_k^{\ell_\alpha,L_\alpha}(\phi_i)\right], \tag{5}$$

where the hyperspherical variables $\rho^2=x_i^2+y_i^2$ and $\cos\phi_i=x_i/\rho$ have been introduced. The pair correlation functions f_α are solutions of a two-body Schrödinger-like equation [10] and are included to accelerate the convergence of the expansion. At small interparticle distances they take into account the correlations introduced by the strong repulsion of the NN potential and go smoothly to unity as the interparticle distance increases. The index α in the sum runs over all the channels compatible with the total angular momentum J value, and the antisymmetrization and parity conditions. In numerical applications the sum is truncated after including all the important channels. The quantities to be determined in the wave function specified by Eqs. (2)–(5) are the hyperradial functions $u_k^\alpha(\rho)$ and the collision matrix elements. They will be calculated by means of the Kohn variational principle.

Below the deuteron breakup the elastic collision matrix is unitary and the problem can be also formulated in terms of the reactance matrix, as done in [8]. Above the deuteron breakup the complex form of the Kohn variational principle [11] is better suited to describe three outgoing particles. In this case, the $\mathcal{S}$-matrix and the hyperradial functions are determined through the stationary value of the functional

$$[{}^J\mathcal{S}_{LL}^{SS}]={}^J\mathcal{S}_{LL}^{SS}+i\langle\Psi^*_{LSJ}|H-E|\Psi_{LSJ}\rangle. \tag{6}$$

Let us first point out the main points of the procedure. After performing the variation with respect to the hyperradial functions, the following set of coupled equations is obtained:

$$\sum_{\alpha',k'}\left[A_{k,k'}^{\alpha,\alpha'}(\rho)\frac{d^2}{d\rho^2}+B_{k,k'}^{\alpha,\alpha'}(\rho)\frac{d}{d\rho}+C_{k,k'}^{\alpha,\alpha'}(\rho)+\frac{m}{\hbar^2}E\ N_{k,k'}^{\alpha,\alpha'}(\rho)\right]u_{k'}^{\alpha'}(\rho)=D_{\alpha k}^{\lambda}(\rho). \tag{7}$$

Details of the explicit form of the coefficients A, B, C, and N and the inhomogeneous term D can be found in Refs. [8,10]. For each asymptotic state ${}^{(2S+1)}L_J$ two different inhomogeneous terms can be constructed in correspondence to the asymptotic Ω_{LSJ}^{λ} functions with $\lambda\equiv$ in or out. Two different sets of hyperradial functions are then obtained by solving the system of equations (7) for the two choices of λ. In the subsequent step the two sets are combined to minimize the functional $[{}^J\mathcal{S}_{LL}^{SS}]$ with respect to variations of the $\mathcal{S}$-matrix elements. This is the first order solution; the second order estimate is calculated by replacing the first order solution in Eq. (6).

Appropriate asymptotic conditions must be imposed on the hyperradial functions $u_k^\alpha(\rho)$ to completely determine the problem. When $\rho\to\infty$, they should vanish below the deuteron breakup threshold, whereas, for positive total energy E, they should be proportional to $\exp(i\sqrt{E}\rho)$. However, this behavior is reached only for very large values of the hyperradius [12], and, in addition, the presence of the Coulomb potential modifies the free outgoing wave also at infinity. Therefore, it is convenient to use the asymptotic behavior of the coefficients A, B, C, N, and D, entering Eq. (7), to obtain the solutions at large but finite ρ. Neglecting terms going to zero faster than ρ^{-3}, the asymptotic expression for the set of differential equations can be cast in the form

$$\sum_{\alpha',k'}\left[\delta_{\alpha,\alpha'}\delta_{k,k'}\left(\frac{d^2}{d\rho^2}-\frac{\mathcal{L}(\mathcal{L}+1)}{\rho^2}+Q^2\right)-\frac{2\ Q\ \chi_{k,k'}^{\alpha,\alpha'}}{\rho}+\frac{h_{k,k'}^{\alpha,\alpha'}}{\rho^3}\right]U_{\alpha'k'}(\rho)=0. \tag{8}$$

The χ term originates from the Coulomb potential matrix elements and it shows the expected $1/\rho$ behavior. The kinetic energy operator and the nuclear potential contribute both to the h term. The final form (8) is obtained after orthonomalizing the PHH states at $\rho=\infty$. In the above equation, $Q^2=mE/\hbar^2$, $\mathcal{L}=\ell_\alpha+L_\alpha+2k+3/2$, and $U_{\alpha k}(\rho)$ are linear combinations of the functions $\rho^{\ell_\alpha+L_\alpha-5/2}u_k^\alpha(\rho)$. The total number of coupled equations in Eqs. (7) and (8) is $N_{\rm eq}$, corresponding to all the considered values of α and k.

For n-d scattering the χ term is zero and, if the coupling term h is neglected, the outgoing solutions of Eq. (8) are the Hankel functions $H^{(1)}(Q\rho)$. In order to take into account the coupling terms, $N_{\rm eq}$ different solutions of Eq. (8) of the kind

$$W_{\alpha k}^{(\alpha_0k_0)}(\rho)=\sum_{\alpha_0',k_0'}\sum_{n=0,1,2,\ldots}\frac{\Gamma_{\alpha k}^{(\alpha_0'k_0')}(n)}{\rho^n}\times(e^{-i\chi\ln2Q\rho})_{\alpha_0',\alpha_0}^{k_0',k_0}e^{iQ\rho}, \tag{9}$$

where χ is the matrix entering Eq. (8), are obtained by choosing $\Gamma_{\alpha k}^{(\alpha_0,k_0)}(n=0)=\delta_{\alpha\alpha_0}\delta_{kk_0}$. The $n>0$ coefficients Γ are determined by recurrence relations obtained from Eq. (8), as done, for example, in Ref. [13].

The solutions of Eq. (7) are then matched to specific superpositions of the functions $W_{\alpha k}^{(\alpha_0k_0)}(\rho)$ by imposing the continuity of the logarithmic derivative at a given value $\rho=\rho_0$. The value of the matching radius ρ_0 is not relevant, provided that the asymptotic form (8) is reached, which is rather well verified for $\rho_0>80$ fm. With such a condition, it has been numerically tested that the solutions are insensitive to variation of ρ_0, even in the presence of Coulomb potential terms. For $\rho\to\infty$, such solutions evolve as

$$U_{\alpha k}(\rho)\to-\sum_{\alpha_0k_0}(e^{-i\chi\log2Q\rho})_{\alpha,\alpha_0}^{k,k_0}S_{\alpha_0k_0}e^{iQ\rho}, \tag{10}$$

corresponding to the correct asymptotic behavior of three outgoing particles interacting via long-range Coulomb potentials [6]. From the above equation, it results that the $S_{\alpha k}$ parameters are just the inelastic $\mathcal{S}$-matrix elements describing the $2\to3$ breakup process. In the n-d case, the hyperradial functions asymptotically reduce to $U_{\alpha k}(\rho)\to-S_{\alpha k}e^{iQ\rho}$.

The NN interaction model considered in the present paper is the s-wave potential of Malfliet and Tjon (MT) [14], with the parameter values given in Ref. [3]. Correspondingly, for

TABLE I. Real parts of the s-wave phase shift ${}^{2S+1}\delta_0$ (in degrees) and inelasticity parameter ${}^{2S+1}\eta_0$ for the doublet and quartet spin states are given as a function of the number N_α of hyperspherical functions considered per channel. The incident nucleon energy is $E_N=14.1$ MeV.

N_α	${}^2\delta_0$	${}^2\eta_0$	${}^4\delta_0$	${}^4\eta_0$
		n-d		
2	97.96	0.5093	67.01	0.9933
4	105.47	0.4652	68.88	0.9788
6	105.51	0.4650	68.94	0.9784
8	105.50	0.4649	68.95	0.9782
		p-d		
2	101.16	0.5430	70.92	0.9905
4	108.41	0.4989	72.53	0.9801
6	108.44	0.4986	72.59	0.9797
8	108.43	0.4985	72.60	0.9795

TABLE II. Results obtained for the real parts of the s-wave phase shift ${}^{2S+1}\delta_0$ (in degrees) and the inelasticity parameter ${}^{2S+1}\eta_0$ are given at the specified incident nucleon energies. For the n-d process, the benchmarks results of Ref. [3] are reported for the sake of comparison.

	${}^2\delta_0$	${}^2\eta_0$	${}^4\delta_0$	${}^4\eta_0$
		n-d at $E_n=14.1$ MeV		
Present	105.50	0.4649	68.95	0.9782
Los Alamos	105.48	0.4648	68.95	0.9782
Bochum	105.50	0.4649	68.96	0.9782
		n-d at $E_n=42.0$ MeV		
Present	41.33	0.5026	37.71	0.9034
Los Alamos	41.34	0.5024	37.71	0.9035
Bochum	41.37	0.5022	37.71	0.9033
		p-d at $E_p=14.1$ MeV		
Present	108.43	0.4985	72.60	0.9795
		p-d at $E_p=42.0$ MeV		
Present	43.65	0.5058	39.94	0.9047

n-d scattering, the function $\Psi_C(\mathbf{x},\mathbf{y})$ defined in Eqs. (3)–(5) includes only $\ell_\alpha=0$ channels. Therefore, the total number of channels for the states with total spin $S=\frac{1}{2}$ ($S=\frac{3}{2}$) is simply 2 (1). On the other hand, the Coulomb potential is active in all the waves, and so, in the p-d case, also channels with angular momenta ℓ_α larger than zero have been included. For central potentials the elastic part of the collision matrix does not depend on J and, moreover, $S=S'$ and $L=L'$. Thus, ${}^J\mathcal{S}^{SS}_{LL}$ has been expressed in the usual form ${}^{2S+1}\eta_L\exp(2i{}^{2S+1}\delta_L)$.

The number of hyperspherical states, i.e., of hyperradial functions, included in each channel has been increased until the convergence is reached. Typically, eight hyperradial functions per channel are enough for a four-digit accuracy in the phase shift parameters. The rate of convergence for the s-wave phase-shifts ${}^2\delta_0$ and ${}^4\delta_0$ and inelasticity parameters ${}^2\eta_0$ and ${}^4\eta_0$ as a function of the number N_α of considered states (equations) per channel α is shown in Table I at $E_N=14.1$ MeV. A similar trend is found at $E_N=42$ MeV and the corresponding converged results are shown in Table II. For n-d scattering a direct comparison with the benchmark results [3] can be done, showing a very good agreement. The phase shift and inelasticity parameters have been also calculated for p-d scattering. Convergence patterns similar to the n-d case are obtained, as can be seen in Table I. Hence, the p-d results are expected to have the same accuracy as the n-d ones. It can be observed that there is a constant difference of about 3° between the p-d and n-d s-wave phase shifts at the energy values considered. A similar difference was obtained by other authors [5,6], using semirealistic potentials.

To compare with experimental results, the elastic cross section has been calculated for several energy values E_N of the incident nucleon. Since the nuclear potential here considered is only s-wave active, the differential cross section starts deviating from the experimental points above $E_N=20$ MeV [1]. For lower E_N values, partial waves up to $L=8$ give sizable contributions and have been included. The calculated n-d elastic cross section is presented in Fig. 1 at neutron energies $E_n=3$, 9, and 18 MeV, together with the experimental data of Ref. [15]. The p-d elastic cross section is given in Fig. 2 at proton energies $E_p=3$, 6, 9, and 18 MeV, in conjunction with the high precision data of Ref. [16]. Despite its simple form, the MT (I–III) potential reproduces the experimental cross sections in a reasonable way. As shown in Ref. [4], the differences found between the theoretical and experimental n-d cross sections are reduced considerably when more realistic NN interactions are used. The same happens in the p-d case at $E_p=3$ MeV [17], and a similar behavior is also expected for higher energies.

The calculation of the breakup cross section is easily performed once the coefficients $S_{\alpha k}$ given in Eq. (10) are

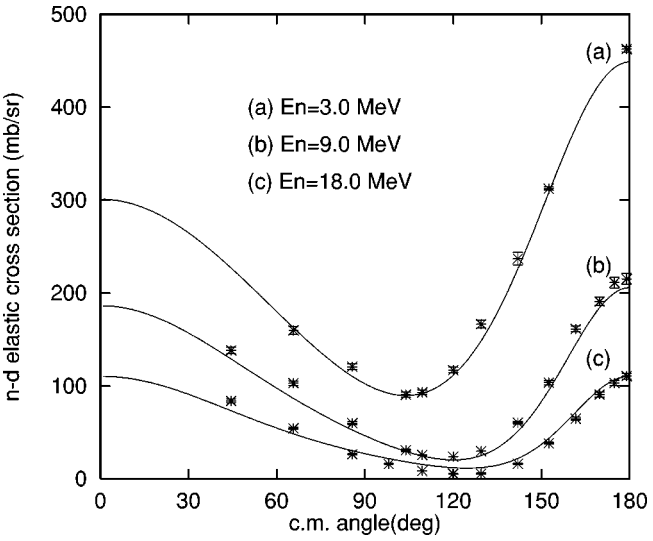

FIG. 1. Elastic n-d cross section at neutron energies $E_n=3$, 9, and 18 MeV. The experimental data are from Ref. [15]

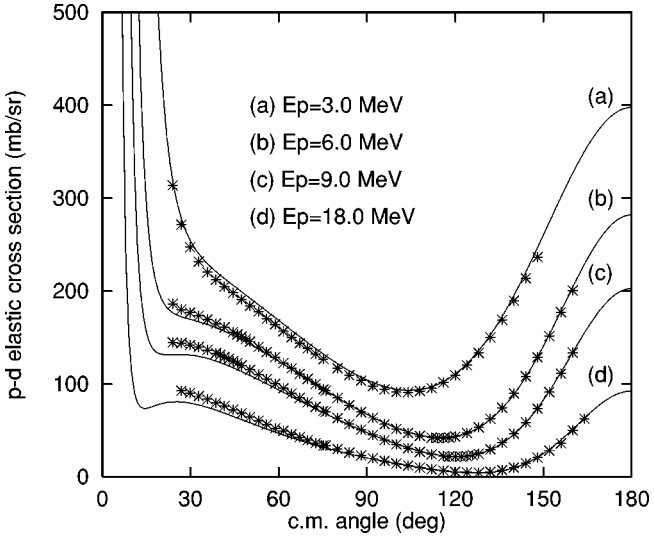

FIG. 2. Elastic p-d cross section at proton energies $E_p = 3$, 6, 9, and 18 MeV. The experimental data are from Ref. [16]

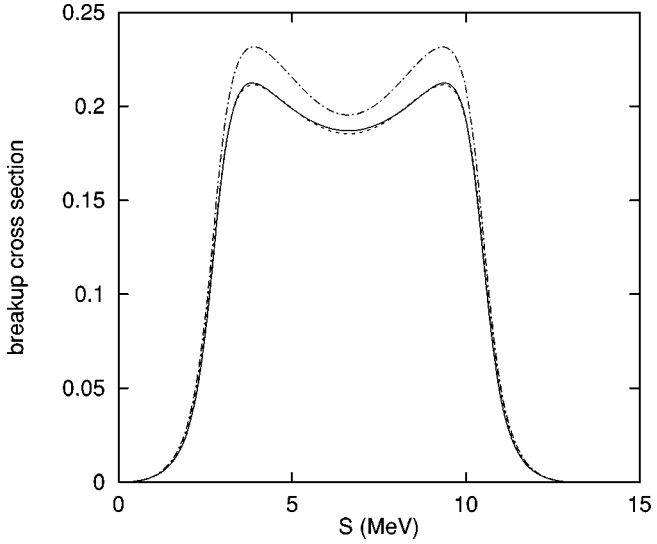

FIG. 3. Laboratory breakup cross section for n-d and p-d scattering at $E_N = 14.1$ MeV versus the arc length S, for the configuration where two neutrons or two protons are detected at angles $\theta_1 = 51.02°$, $\theta_2 = 51.02°$, and $\varphi = 120°$. For the sake of comparison with the calculation of Ref. [3], only the contributions from s waves have been included. The solid (dot-dashed) curve corresponds to n-d (p-d) scattering. The dashed curve shows the n-d results of Refs. [3,18].

known. The $\mathcal{S}$-matrix unitarity imposes the following relation between the elastic and inelastic parameters:

$$|^{2S+1}\eta_L|^2 + \sum_{\alpha k} |S_{\alpha k}|^2 = 1. \tag{11}$$

In all the cases we have considered, this relation is well verified numerically with a precision of 10^{-5}. An example of n-d and p-d breakup cross sections, for the space star configuration, is reported in Fig. 3. For the sake of comparison, the n-d breakup cross section calculated by means of the Faddeev technique [3,18] is reported, as well. All the cross sections reported are calculated by including the contribution of s waves only. From inspection of Fig. 3, it can be noticed that there is good agreement between the results of the two n-d calculations. In fact, the present estimation is found to differ by 1% at most from the benchmark result of Ref. [3]. This difference should be further reduced by increasing the number of PHH states included in the expansion.

The p-d cross section shown in Fig. 3 is found to be larger than that of the corresponding n-d scattering, in contrast to the experimental data where the inverse situation is observed [19,20]. In Ref. [21], where the interaction used was a Yamaguchi separable potential and the Coulomb effect was treated with some approximation, the p-d space star cross section was found to be slightly smaller than the n-d one. However, the n-d breakup cross section shown in Fig. 3 of the present paper is about 5 times smaller than the experimental value. For the simple potential used here there are some cancellations in the construction of the breakup cross section in this particular configuration. These cancellations are found to be less effective when the Coulomb potential is included. It should also be observed that the contributions of the $L > 0$ waves were not included in the cross section presented in Fig. 3. In conclusion, the interesting problem is to investigate the effect of the Coulomb potential in the case of realistic interactions. In this respect, in Ref. [4], the n-d space star cross section was calculated using the Bonn nucleon-nucleon potential, which resulted in being slightly smaller than the experimental n-d value.

The inelasticity parameter $^{2S+1}\eta_L$ goes to one as L increases, as, for example, has been found in Refs. [1,4] for n-d scattering. For instance, at $E_n = 14.1$ MeV, $(1 - {}^{2S+1}\eta_L) < 10^{-3}$ already for $L \geq 4$. A similar behavior has been found for the p-d case. The contributions to both elastic and inelastic cross sections of channels with $\ell_\alpha > 0$, included in the p-d case, have been found to be nearly negligible.

We conclude with a few remarks. First of all, the Kohn variational principle has been successfully applied to treat scattering processes above the deuteron breakup threshold. The complex form of the principle is well suited to take into account the boundary conditions for the three outgoing nucleons and to obtain the second order estimate of the $\mathcal{S}$-matrix. The expansion of the wave function in the PHH basis allows for lowering the number of hyperspherical states to be included. The problem reduces to the solution of a set of second-order inhomogenous differential equations with outgoing boundary conditions. For p-d scattering the equations are coupled even in the asymptotic region due to the Coulomb potential. However, a simple technique can be used to calculate the proper boundary conditions for the wave function at values of the hyperradius $\rho \approx 100$ fm. The results obtained for the complex s-wave n-d phase-shift parameters are in complete agreement with the benchmark calculations of Ref. [3]. The elastic cross sections have been compared with the experimental data. For both processes, n-d and p-d, an overall good agreement has been observed. The differences found may be ascribed, in large part, to the rather simple potential used.

The extension of the method to realistic NN interactions will be the subject of a subsequent paper.

[1] W. M. Kloet and J. A. Tjon, Ann. Phys. (N.Y.) **79**, 407 (1973); Nucl. Phys. **A210**, 380 (1973).
[2] J. L. Friar *et al.*, Phys. Rev. C **42**, 1838 (1990).
[3] J. L. Friar *et al.*, Phys. Rev. C **51**, 2356 (1995).
[4] W. Glöckle, H. Witala, D. Hüber, H. Kamada, and J. Golak, Phys. Rep. **274**, 107 (1996).
[5] E. O. Alt, W. Sandhas, and H. Ziegelmann, Nucl. Phys. **A445**, 429 (1985); E. O. Alt and M. Rauh, Few-Body Syst., Suppl. **7**, 160 (1994).
[6] S. P. Merkuriev, Ann. Phys. (N.Y.) **130**, 395 (1980); Yu. A. Kuperin, S. P. Merkuriev, and A. A. Kvitsinskii, Sov. J. Nucl. Phys. **37**, 857 (1983).
[7] H. van Haeringen and R. van Wageningen, J. Math. Phys. **16**, 1441 (1975).
[8] A. Kievsky, M. Viviani, and S. Rosati, Nucl. Phys. **A577**, 511 (1994).
[9] A. Kievsky, M. Viviani, and S. Rosati (unpublished).
[10] A. Kievsky, M. Viviani, and S. Rosati, Nucl. Phys. **A551**, 241 (1993).
[11] J. Z. H. Zhang, S. Chu, and W. H. Miller, J. Chem. Phys. **88**, 6233 (1988); R. R. Lucchese, Phys. Rev. A **40**, 687 (1989).
[12] W. Glöckle and G. L. Payne, Phys. Rev. C **45**, 974 (1992).
[13] M. I. Haftel and V. B. Mandelzweig, Ann. Phys. (N.Y.) **150**, 48 (1983).
[14] R. A. Malfliet and J. A. Tjon, Nucl. Phys. **A127**, 161 (1969).
[15] P. Schwartz *et al.*, Nucl. Phys. **A398**, 1 (1983).
[16] K. Sagara *et al.*, Phys. Rev. C **50**, 576 (1994).
[17] A. Kievsky, S. Rosati, W. Tornow, and M. Viviani, Nucl. Phys. **A607**, 402 (1996).
[18] H. Witala and W. Glöckle (private communication).
[19] J. Strate *et al.*, Nucl. Phys. **A501**, 51 (1989).
[20] G. Rauprich *et al.*, Nucl. Phys. **A535**, 313 (1991).
[21] E. O. Alt and M. Rauh, Phys. Rev. C **49**, R2285 (1994).